Polymer 52 (2011) 1755–1765

Contents lists available at ScienceDirect

Polymer

journal homepage: www.elsevier.com/locate/polymer

Novel amphiphilic diblock copolymers bearing acid-labile oxazolidine moieties: Synthesis, self-assembly and responsive behavior in aqueous solution

Qianling Cui [a,b], Feipeng Wu [a,*], Erjian Wang [a]

[a] Technical Institute of Physics and Chemistry, Chinese Academy of Sciences, Beijing 100190, PR China
[b] Graduate University of Chinese Academy of Sciences, Beijing 100049, PR China

ARTICLE INFO

Article history:
Received 27 October 2010
Received in revised form
30 December 2010
Accepted 16 February 2011
Available online 23 February 2011

Keywords:
Amphiphilic diblock copolymers
pH-responsivity
RAFT polymerization

ABSTRACT

A novel oxazolidine based acid-labile monomer *N*-acryloyl-2,2-dimethyl-1,3-oxazolidine (ADMO) was synthesized and polymerized by reversible addition fragmentation chain transfer (RAFT) polymerization using poly(ethylene glycol) based chain transfer agent (PEG-CTA). The diblock copolymers PEG-*b*-PADMO were composed of hydrophilic PEG with fixed length and hydrophobic PADMO with different lengths, which formed core-shell micelles in water. Morphologies and sizes of micelles were obtained by transmission electron microscopy (TEM) and dynamic light scattering (DLS), which showed that the shapes of polymeric aggregates developed from small spherical micelles, worm-like micelles to larger size of vesicles, as the length of PADMO increased. The hydrolysis kinetics of the micelles was studied using ^{1}H NMR, DLS and release of loaded Nile Red dye, whose rate strongly depended on pH and micellar structure. It led to the disruption of polymeric micelles and concomitant release of the guest molecules, due to the transformation of hydrophobic PADMO into hydrophilic poly(2-hydroxyethyl acrylamide) (PHEAM).

1. Introduction

Stimuli-responsive polymers have attracted growing interests in recent years, due to their potential applications in fields such as catalysis, drug and gene delivery, separation and purification of biomolecules and biosensor etc [1–3]. Amphiphilic block copolymers with stimuli-responsive elements are of particular importance. These copolymers self-assemble in solution into various ordered structures such as spherical micelles, worm-like or cylindrical micelles, and vesicles, controlled by the ratio of the block lengths, polymer concentration, temperature, additives and other factors [4–8]. Polymeric micelles have several advantages, such as unique core-shell architecture, which provides interiors that can non-covalently encapsulate guest molecules. The micelles, with average size typically between 20 and 100 nm, can accumulate the drug at target sites via an enhanced permeation and retention (EPR) effect [9]. In addition, the polymeric micelles are easily prepared, and provide design flexibility for controlling nanostructure and functionality [10–12]. Based on this concept, many stimuli-responsive polymeric micelle systems have been designed and prepared based on amphiphilic block copolymers, which can change their physical or chemical properties in response to external stimuli such as pH [13], temperature [14,15], ionic strength [16], light [17], redox potential [18,19] and other environmental variables.

The pH-sensitive polymers are among the most important stimuli-responsive materials. They are of particular interest for biomedical and biotechnological applications, since there are numerous pH gradients existing in both normal and pathological states, which provide a potential localized trigger for the release of drugs from acid-sensitive carriers [20]. According to the difference of response mechanism, pH-sensitive polymers can be classified into two types. Typical pH-sensitive polymers contain reversible ionizable segments such as polyacids and polybases [21,22], whose properties change reversibly by protonation or deprotonation as the pH of the surroundings changes. Another strategy for preparation of pH-sensitive polymers is introducing acid-labile linkages or moieties such as acetals [23–30], orthoesters [31–35], hydrazones [36–38], anhydrides [39] and others [40,41] into the polymer main or side chain. Acid-catalyzed cleavage of these linkers induces disruption of the micelles or vesicles and consequential release of loaded guests. Kataoka et al. [42,43] prepared polymeric micelles by attaching doxorubicin (DOX) to amino acid units of PEG-*b*-P(Asp) via hydrazone linkages. Park and coworkers [44] reported a block copolymer (PEG-*b*-PLLA) with terminal conjugated DOX through a hydrazone or *cis*-acotinyl bond. These acid-sensitive micelles had much faster release of free DOX at acid pHs than at neutral pH.

* Corresponding author. Tel.: +86 10 82543569; fax: +86 10 82543491.
E-mail address: fpwu@mail.ipc.ac.cn (F. Wu).

0032-3861/$ – see front matter © 2011 Elsevier Ltd. All rights reserved.
doi:10.1016/j.polymer.2011.02.022

The acetals and orthoesters are two kinds of widely used acid-sensitive linkages for pH-responsive micelles or other nanoparticles, whose hydrolysis are generally proportional to the hydronium ion concentration and the products are diol and ketal [45]. Their hydrolysis rates can be designed and controlled by the degree of substitution and substituent structure [46]. Fréchet and coworkers [23] provided an approach to acid-sensitive micelles by attaching hydrophobes to one block of diblock copolymers via an acetal linkage. Since common aliphatic acetals generally hydrolyze slowly, the introduction of benzylidene acetals with electron-donating methoxy groups in the *ortho* and *para* positions accelerated the hydrolysis rate, which increased rapidly as the pH changed from 7.4 to 5.0. However, the aromatic hydrolysis product is not a biocompatible and biodegradable material. This problem has been avoided in several studies [47–49]. For example, Li and coworkers [47] prepared the new monomer *N*-(2,2-dimethyl-1,3-dioxan-5-yl) (meth)acrylamide and corresponding acid-sensitive polymers containing pendant cyclic acetal groups. The degradation products in that case were neutral diols and acetals, thus eliminating the inflammation problems, but the hydrolysis rate of this six-membered cyclic acetal was quite slow. It was known that cyclic orthoesters were hydrolyzed about two orders of magnitude faster than cyclic acetals [46]. For that reason, Li's group also prepared polymers or diblock copolymers bearing six-membered cyclic orthoester groups [48–50], which were found to hydrolyze mainly through two paths, including endocyclic and exocyclic cleavage, giving rise to a mixture of side chain structures. Heller [51] and Tang [52] reported another type of pH-responsive nanoparticles assembled from amphiphilic diblock copolymers bearing a hydrophobic five-membered cyclic orthoester as pendant groups. Hydrolysis of these orthoester moieties followed a distinct exocyclic mechanism and produced water soluble polymeric formate and a small molecule carbonyl compound. Although the hydrolysis rate of cyclic orthoesters was faster, the acidic degradation products frequently inhibited their in vivo application. To develop a new type of acid-labile linkage that is environment friendly and biocompatible is still an important task for chemists.

Oxazolidines are highly pH-sensitive molecules that can be regarded as cyclic acetal analogs with one oxygen atom replaced by nitrogen, and have been widely used for protection of β-amino alcohols for asymmetric synthesis [53] and used as prodrug forms [54]. These heterocycles have been found to undergo a facile and complete hydrolysis in a wide pH range, producing the corresponding carbonyl compound and β-amino alcohol [55]. The hydrolysis capacity of the oxazolidine can be adjusted by introducing functional groups on the nitrogen atom [56]. Since β-amino alcohols and/or carbonyl-containing compounds are widely found in the biological and pharmaceutical sciences, this category of oxazolidines could be used as another kind of excellent acid-labile group, in addition to cyclic acetals and orthoesters, to construct novel pH-sensitive polymeric micelles. To the best of our knowledge, there have been no reports on polymeric micelles involving the oxazolidines.

In this work, the oxazolidine based monomer *N*-acryloyl-2,2-dimethyl-1,3-oxazolidine (ADMO) was synthesized as well as its homopolymer (PADMO), which was readily hydrolyzed in mildly acidic media, producing the parent compound HEAM (or PHEAM), while stable in neutral and basic aqueous solution. Based on the acid-labile oxazolidine type monomer (ADMO), a series of novel pH-responsive amphiphilic diblock copolymers PEG-*b*-PADMO was designed and synthesized by RAFT polymerization. The copolymers were composed of hydrophilic PEG blocks and polyacrylamide segments of varying length with pendant oxazolidine moieties. The micellization and stimuli-responsive behavior of the copolymers in aqueous solution were studied using ^{1}H NMR spectroscopy, DLS, TEM measurements, fluorescence probe technique and release of encapsulated Nile Red dye.

2. Experimental section

2.1. Materials

2-Hydroxyethyl acrylamide (HEAM, Sigma Aldrich), 2,2-dimethoxypropane (DMP, Alfa Aesar), poly(ethylene glycol) monomethyl ether (PEG, M_n = 2010 g mol^{-1}, BASF), Nile Red (NR, Alfa Aesar) were used without further purification. *p*-Toluenesulfonic acid monohydrate (*p*-TSA), *N*,*N*′-dicyclohexyl carbodiimide (DCC), and 4-dimethylaminopyridine (DMAP) were purchased from Aladdin Reagent Company (Shanghai, China). 4-Cyanopentanoic acid dithiobenzoate (CPDB) was synthesized according to the literature procedure [57]. 2,2′-Azobis(isobutyronitrile) (AIBN) was recrystallized twice from ethanol and stored in the refrigerator. Tetrahydrofuran (THF) was purified by distillation from sodium with benzophenone, and 1,4-dioxane was distilled over CaH_2 prior to use. DCl (20% in D_2O solution) and other deuterated solvents (99.8% purity) were purchased from Beijing Seaskybio Company. Other solvents and reagents were purchased from Beijing Chemical Reagent Company, and used as received. All the aqueous solutions were prepared using deionized water.

2.2. Synthesis of N-acryloyl-2,2-dimethyl-1,3-oxazolidine (ADMO) monomer

2-Hydroxyethyl acrylamide (14.4 g, 0.12 mol), 2,2-dimethoxypropane (18.4 mL, 0.15 mol), and *p*-TSA (0.09 g, 0.48 mmol) were dissolved in 250 mL anhydrous THF. The reaction mixture was stirred at ambient temperature for 24 h. After removing most part of the solvent by a rotary evaporator, the residue was purified by silica gel column chromatography using hexane/ethyl acetate (4/1, v/v) as the eluent, to afford clear colorless oil and the yield was ~46%. ^{1}H NMR ($CDCl_3$, δ, ppm): 1.61 (s, 6H, -C(CH_3)$_2$), 3.68 (t, 2H, -N−CH_2−), 4.02 (t, 2H, −CH_2−O−), 5.67 (dd, 2H, CH_2= CH−), 6.38 (d, 4H, CH_2= CH−). ^{13}C NMR ($CDCl_3$, δ, ppm): 24.3 (−C(CH_3)$_2$), 46.0 (N−CH_2−CH_2−), 63.0 (−CH_2−CH_2−O−), 94.7 (−C(CH_3)$_2$), 127.7 (CH_2= CH−), 129.6 (CH_2= CH−), 162.2 (−C=O). HR-MS (ESI): calcd for $C_8H_{13}NO_2$ [M + Na]$^+$: 155.08385, found: 178.08426.

2.3. Synthesis of poly(ethylene glycol)-based chain transfer agent (PEG-CTA)

PEG-CTA was synthesized according to the literature procedure [58]. PEG (13 g, 6.5 mmol), CPDB (2.3 g, 8.2 mmol), and a trace of 4-dimethylaminopyridine (DMAP) were dissolved in 50 mL CH_2Cl_2 solution. This mixture was added by a CH_2Cl_2 solution (50 mL) of *N*,*N*′-dicyclohexyl carbodiimide (DCC) (2.8 g, 13.7 mmol) over 30 min. After stirred for 20 h in oil bath at 40 °C, the mixture was filtrated to remove dicyclohexylurea. The solvent was removed, and the residue was purified by silica gel column chromatography using $CHCl_3$ as the eluent, followed by a mixture of $CHCl_3$ and CH_3OH (95/5, v/v). The product was dried under vacuum at room temperature for 24 h, obtained as red solid with a yield 52.3%. ^{1}H NMR ($CDCl_3$, δ, ppm): 1.93 (s, 3H, CH_3−C-CN), 2.55 (m, 2H, −CH_2−CH_2−C−CN), 2.75(m, 2H, −CH_2−CH_2−C-CN), 3.37 (s, 3H, PEG−OCH_3), 3.45–3.75 (m, PEG backbone), 3.81 (t, 2H, −CH_2−CH_2−OOC−), 4.27 (t, 2H, −CH_2−CH_2−OOC−), 7.39–7.89 (5H, −C_6H_5).

2.4. Synthesis of poly(ethylene glycol)-block-poly(N-acryloyl-2,2-dimethyl-1,3-oxazolidine) (PEG-b-PADMO)

As shown in Scheme 3, diblock copolymers were synthesized via reversible addition fragmentation chain transfer polymerization (RAFT) using PEG-CTA as macro RAFT agent. To obtain diblock copolymers with different PADMO block lengths, the molar ratio

of monomer to CTA was varied at 20, 30, 50, and 100 respectively. As an example, for synthesis of copolymer with PADMO length of 30 units, ADMO (0.7 g, 4.5 mmol), PEG-CTA (0.375 g, 0.15 mmol) and AIBN (2.5 mg, 0.015 mmol) were dissolved in 5 mL 1,4-dioxane. The solution was deoxygenated by purging with nitrogen gas for 30 min. Polymerization was carried out in water bath at 70 °C for 24 h, and terminated by ice bath and exposure to air. The polymer was isolated by three times re-precipitations from THF to hexane and dried under vacuum at room temperature for 24 h, obtained as a pink powder. ^{1}H NMR ($CDCl_3$, δ, ppm): 1.55 (−C(CH_3)$_2$), 1.10–3.00 (−(CH_2−CH)−), 3.38 (PEG-OCH_3), 5.61 (PEG), 3.00–4.40 (−N−CH_2−CH_2−O−), 7.39–7.89 (−C_6H_5).

2.5. Synthesis of homopolymer poly(N-acryloyl-2,2-dimethyl-1,3-oxazolidine) (PADMO)

Homopolymer PADMO was prepared by traditional radical polymerization as follows: ADMO (0.78 g, 5 mmol), AIBN (1.6 mg, 0.01 mmol) were dissolved in 10 mL 1,4-dioxane. The solution was deoxygenated by purging with nitrogen gas for 30 min. Polymerization was carried out in water bath at 60 °C for 12 h. The polymer was subsequently purified by precipitation into hexane and obtained as a white powder. ^{1}H NMR ($CDCl_3$, δ, ppm): 1.55 (−C(CH_3)$_2$), 1.10–2.05 (−(CH_2−CH)−), 2.05–3.00 (−(CH_2−CH)−), 3.15–4.30 (−N−CH_2−CH_2−O−).

2.6. Characterization methods

^{1}H NMR (400 MHz) and ^{13}C NMR (400 MHz) spectra were recorded on a Bruker DPX-400 NMR spectrometer in the deuterated solvents at 25 °C, using tetramethylsilane (TMS) as an internal standard.

The high resolution mass spectrometer (HR-MS, ESI) analyses were carried out on a Bruker apex IV FT mass spectrometer.

The molecular weights and molecular weight distributions of polymer were estimated by gel permeation chromatography (GPC) on equipment composed of a Waters 1525 binary HPLC pump, a Waters 2414 refractive index detector, and three Waters Styragel columns. THF was used as eluent at a flow rate of 1.0 mL min^{-1}, and linear polystyrene standard was used for calibration.

Transmission electron microscopy measurements (TEM) were conducted on a JEOL JEM-2100 transmission electron microscope with an accelerating voltage of 200 kV. The sample was prepared by placing a drop of the copolymer solution onto a carbon-coated copper grid (400 mesh), staining with 1% (w/v) uranyl acetate solution, and allowing the sample to dry in air before measurement.

Average hydrodynamic radius and distributions of the aggregates formed in polymer aqueous solution were measured by DynaPro NanoStar instrument (Wyatt Technology), with a He−Ne laser ($\lambda = 658$ nm) operated at 10 mW. The measurements were made at the scattering angle $\theta = 90°$ at 25 °C, and the samples were purified by Millipore filters with 0.45 μm pore size before the measurements.

2.7. Preparation of aqueous micelle solutions

The micelle solutions of the block copolymers were prepared by dissolving the polymers in water directly except sample $E_{45}A_{88}$, which was treated by dialysis method. The sample $E_{45}A_{88}$ was first dissolved in THF, and water was then added slowly into the solution to induce the formation of micelles. The solution was stirred for 2 h at room temperature before being placed in a dialysis bag (MW cutoff 3500 Da) for dialysis against water for three days (water was frequently refreshed).

2.8. Determination of critical aggregates concentration (CAC)

Critical aggregates concentrations (CAC) of the copolymers were estimated by a fluorescence spectroscopic method using pyrene as the fluorescence probe. 200 μL of pyrene in methanol solution (5.0×10^{-5} mol L^{-1}) was added into a series of 10 mL volumetric flasks, and the solvent was then evaporated completely. A series of copolymer aqueous solutions at different concentrations ranging from 1.0×10^{-4} to 1.0 mg mL^{-1} were added to the bottles, whereas the final concentration of pyrene in each flask was 1.0×10^{-6} mol L^{-1}. The excitation spectra of pyrene were obtained on a Hitachi F-4500 fluorescence spectrometer, from 300 to 350 nm with the emission wavelength at 383 nm. The value of CAC was determined from the plots of the intensity at 338 and 333 nm against the polymer concentration.

2.9. Determination of the hydrolysis rate

For the measurement of the monomer, ADMO was dissolved in 0.5 mL D_2O, and pH was adjusted to 3.0, 5.0, and 7.4, by addition of 20 μL of 5.0 M pH 3.0, 5.0 acetate buffer or 7.4 phosphate buffer. For pH 2.0, the solution was adjusted by 5 M HCl. The ^{1}H NMR spectra were recorded at different time points. For the polymer, the micelles solution in D_2O with a concentration 5 mg mL^{-1} was added by 50 μL DCl (20% in D_2O solution), and measured by ^{1}H NMR at predetermined time.

2.10. Encapsulation and release of Nile Red

200 μL of Nile Red in dichloromethane solution (5.0×10^{-5} mol L^{-1}) was added into a 10 mL volumetric flask, and the solvent was then evaporated completely. The polymer aqueous solution (0.2 mg mL^{-1}) was added to the bottle, whereas the final concentration of Nile Red was 1.0×10^{-6} mol L^{-1}. The solution was placed overnight to reach the equilibrium. 2 mL solution was adjusted to pH 3.0, 5.0, and 7.4, by addition of 50 μL of 5.0 M pH 3.0, 5.0 acetate buffer or pH 7.4 phosphate buffer. The samples were incubated at 37 °C and the fluorescence intensity was measured at the desired time points. The excited wavelength was set at 550 nm, and slit widths were maintained at 5.0 nm.

3. Results and discussion

3.1. Synthesis and characterization of acid-labile monomer ADMO

The novel acid-labile monomer *N*-acryloyl-2,2-dimethyl-1,3-oxazolidine (ADMO) was synthesized from 2-hydroxyethyl acrylamide (HEAM) and 2,2-dimethoxypropane (DMP) in the presence of *p*-toluenesulfonic acid (*p*-TSA) as catalyst, involving condensation and cyclization (Scheme 2a). The new monomer was stable at room temperature and easily soluble in common organic solvents and water. The chemical structure and configuration of ADMO was confirmed by ^{1}H NMR, ^{13}C NMR spectroscopy and HR-MS (ESI) analysis.

From the ^{1}H NMR spectrum of ADMO, the difference in the doublet peaks at 1.55–1.61 ppm in D_2O and $CDCl_3$ solutions of ADMO indicated that the monomer comprised diastereomeric mixtures of rotational isomers, as shown in Fig. 1a and Fig. S1. However, the *trans* isomer Z was predominantly excess over the *cis* isomer E, in which the unfavorable steric interactions existed, especially the dimethyl substitution created an even greater affection. Indeed, solvent effect was evident as illustrated in ^{1}H NMR spectra by the higher Z isomer populations in D_2O than in $CDCl_3$ [59]. Since this work did not focus on the stereochemistry of

the monomer and the polymer, these aspects were not further investigated.

Since the oxazolidines exhibit n(N) → σ*(C—O) electron delocalization and are sensitive to a wide range of pHs, electron withdrawing or electron-donating groups attached to the nitrogen atom would be expected to affect the reactivity of the five-membered ring. It has been proved that when the nitrogen lone pair is conjugated with a carbonyl group (n(N) → π(C═O) electron delocalization) as in *N*-acryloyl oxazolidines, both hydrolysis and reductive ring—opening reactions become much more difficult, as a consequence of a concomitant decrease of oxygen basicity and increase of the intra-cyclic C—O bond strength. Thus their ring—opening reactions require the presence of a strong oxophilic catalyst (proton or Lewis acid) [56]. The monomer ADMO, containing an *N*-substituted carbonyl moiety, was found by thin layer chromatography (TLC) and ^{1}H NMR spectroscopy to undergo facile hydrolysis under acidic catalysis while being stable in neutral or basic medium for a long time.

Fig. 1 shows ^{1}H NMR spectra of ADMO before and after addition of DCl to the D_2O solution of the monomer. The peak at 1.55 ppm, assigned to the dimethyl group protons of ADMO, significantly reduced after 20 μL DCl was added, and disappeared after 0.5 h. Concomitantly, a new peak at 2.10 ppm, assigned to the byproduct acetone, increased rapidly with time. According to previous studies, oxazolidine hydrolysis occurs in two stages: reversible ring opening through C—O bond cleavage to give a cationic Schiff base species, followed by hydrolysis of this intermediate to give the β-amino alcohol and the carbonyl component [54]. Thus, the hydrolysis mechanism of ADMO monomer can be described as shown in Scheme 2b.

The kinetics of hydrolysis of ADMO was further studied in aqueous solution at different pH values at 25 °C using ^{1}H NMR spectroscopy. The degree of hydrolysis was estimated by monitoring the change of the ratio of intensities of the signal at 2.10 ppm, which was ascribed to the released acetone protons, to the signal at 1.55 ppm of the dimethyl protons of oxazolidine group. As seen in Fig. 2, the hydrolysis of ADMO displayed strict first order kinetics and strong pH dependence. The hydrolysis rate constants and half-lives were calculated from the slopes of the linear plots. At pH 5.0, hydrolysis proceeded very slowly. The hydrolysis rate increased rapidly with decreasing pH, with half-life 44 h at pH 3.0 and 4.5 h at pH 2.0.

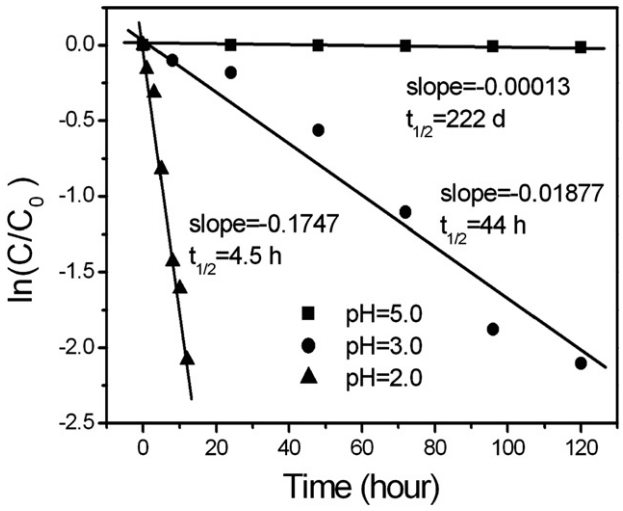

Fig. 2. Hydrolysis kinetics of acid-labile monomer ADMO at different pHs at 25 °C.

ADMO monomer, being an acrylamide derivative, was found to easily undergo free radical polymerization. The homopolymer PADMO was soluble in common organic solvents including acetone, tetrahydrofuran, ethanol, methanol, ethyl acetate, chloroform, toluene, 1,4-dioxane, dimethylsulfoxide and *N*,*N*-dimethylformamide, but insoluble in hexane and water. At low pH, the homopolymer was readily converted from hydrophobic PADMO to hydrophilic PHEAM (Scheme 1) via hydrolysis of oxazolidine pendant groups, displaying the expected effective acid stimuli-responsiveness. Thus PADMO showed similar pH-responsive behavior to that of acid-sensitive polymers containing cyclic orthoesters [51,52] and acetals [23].

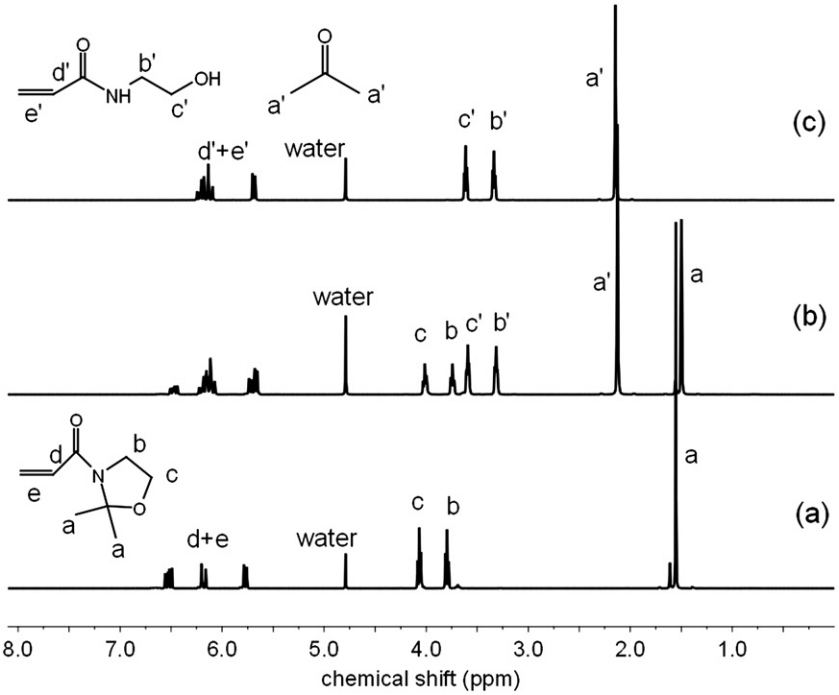

Fig. 1. ^{1}H NMR spectra of ADMO monomer before and after addition of DCl to its solution in D_2O. (a) 0 min, (b) 5 min, and (c) 0.5 h.

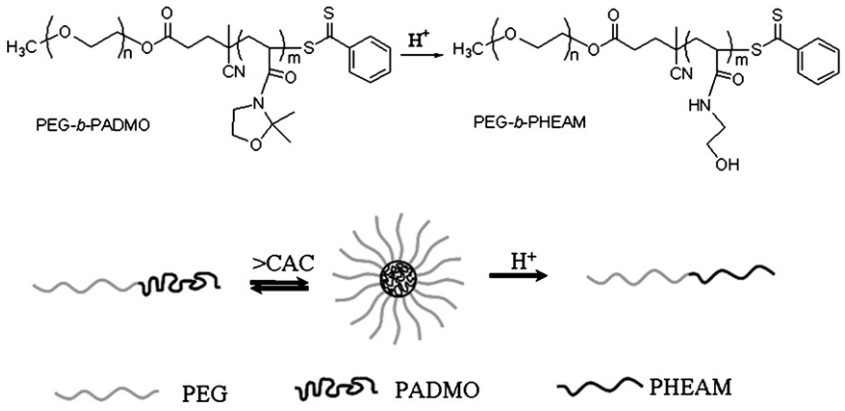

Scheme 1. Schematic representation of the functional aggregation behavior of the pH-responsive diblock copolymer PEG-*b*-PADMO.

3.2. Synthesis and characterization of diblock copolymers

Diblock copolymers PEG-*b*-PADMO with well-defined structures, consisting of hydrophilic PEG part and hydrophobic PADMO part, were prepared via RAFT controlled radical polymerization of functional monomer ADMO using PEG-based macromolecular chain transfer agent (PEG-CTA) and initiator AIBN, as shown in Scheme 3. PEG-CTA was synthesized via esterification of the terminal hydroxyl group of poly(ethylene glycol) monomethyl ether (M_n = 2010 g mol^{-1},) with 4-cyanopentanoic acid dithiobenzoate (CPDB), a chain transfer agent commonly used in RAFT polymerization of (methyl)acrylamide monomers [57,60], in the presence of DCC and DMAP catalysts. The structure of the product was supported by ^{1}H NMR spectra, in accordance with that previously reported [58]. The RAFT functionality of PEG-CTA was calculated to be 95% based on the data of ^{1}H NMR spectra, and the impurity may include the residual PEG and dead products from side reactions [61,62].

A series of PEG-*b*-PADMO diblock copolymers with PADMO blocks of varying length and PEG blocks with fixed length were obtained as listed in Table 1, using different feed ratios of initial concentration of monomer to CTA ($[M]_0/[CTA]_0$), ranging from 20, 30, 50 to 100 respectively, at a constant ratio ($[CTA]_0/[I]_0$) of 10:1. The polymers obtained were soluble in common organic solvents except hexane, and soluble in water (except for sample $E_{45}A_{88}$).

The molecular weights of the copolymers were determined by theoretical and experimental methods. The synthesis details and characterization data for various PEG-*b*-PADMO diblock copolymers are summarized in Table 1. The targeted number average molecular weight $M_{n(theor)}$ was calculated based on a simplified formulation as follows [61,63]: $M_{n(theor)} \cong (N_{theor} \times M_{ADMO} \times [M]_0/[CTA]_0) + M_{CTA}$, where N_{theor} is the targeted degree of polymerization, $[M]_0$ is the initial concentration of monomer, M_{ADMO} is the molecular weight of ADMO monomer, $[CTA]_0$ is the initial concentration of PEG-CTA, and M_{CTA} is the molecular weight of PEG-CTA. Considering the high conversion (>95%) for ADMO polymerization in the given experiment condition, which was determined by ^{1}H NMR method (shown in Supplementary data Fig. S8). It is reasonable to calculate $M_{n(theor)}$ within the permit error range on the assumption of complete conversion (N_{theor} = 100%). The theoretical molecular weight $M_{n(theor)}$ for different copolymer samples are listed in Table 1.

From the ^{1}H NMR spectra of the block copolymers in $CDCl_3$, $M_{n(NMR)}$ was obtained by comparing the integrated signals of the protons of the dimethyl groups plus polyacrylamide backbones at 1.30–3.00 ppm, with those of the signals at 3.10–4.50 ppm corresponding to the sum of PEG (3.45–3.75 ppm) and methylene protons on the five-membered ring of PADMO. The numbers of ADMO repeating units in the different length diblock copolymer samples were estimated to be 18, 28, 47 and 88, close to the feed compositions. The corresponding copolymers are denoted as $E_{45}A_{18}$, $E_{45}A_{28}$, $E_{45}A_{47}$, and $E_{45}A_{88}$, where E and A represents PEG and PADMO block respectively. The $M_{n(NMR)}$ values (Table 1) for the block copolymers were in fair agreement with the $M_{n(theor)}$ values.

As an alternative method, molecular weights were also estimated by GPC. Fig. 3 shows GPC elution curves for PEG-CTA and the diblock copolymers. As polymer growth increased with the $[M]_0/[CTA]_0$ ratio, the peak of the corresponding copolymer shifted toward lower retention time (higher molecular weight). All GPC traces presented a monomodal, narrow molar mass distributions

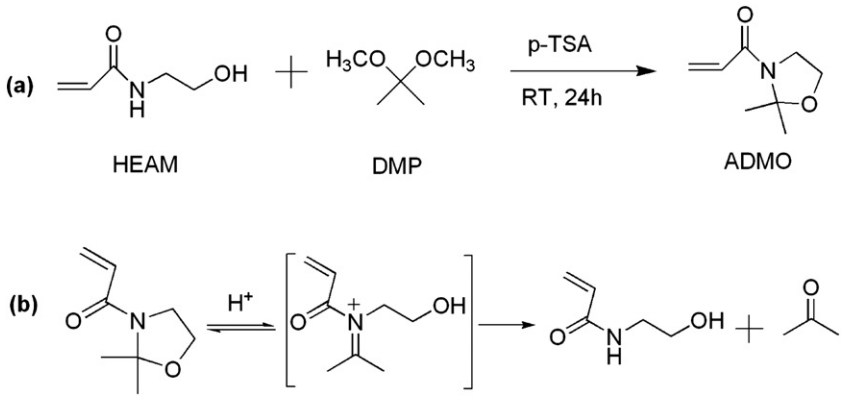

Scheme 2. Synthetic pathway (a) and hydrolysis mechanism (b) for the monomer ADMO.

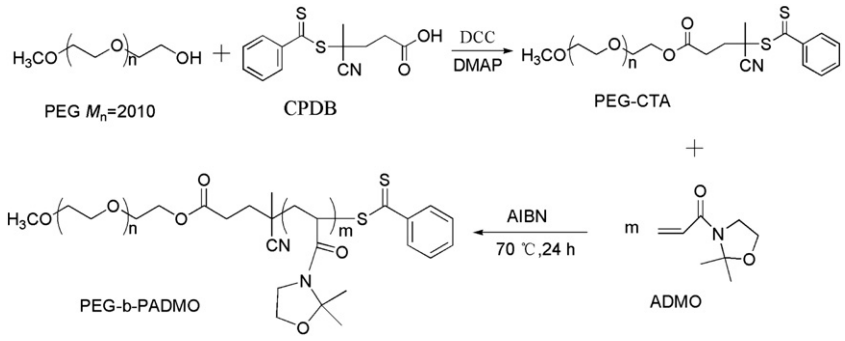

Scheme 3. Synthesis routes of PEG-CTA and diblock copolymer PEG-*b*-PADMO.

with polydispersity indexes (M_w/M_n) from 1.13 to 1.19, demonstrating efficient polymerization control with the RAFT agent PEG-CTA. It should be noted that the GPC traces for the copolymers exhibited a small shoulder on the low molar mass side, which is corresponding to the position of PEG-CTA curve, suggesting minor contamination of the original macro RAFT agent. Since the RAFT functionality of PEG-CTA synthesized was determined to be 95% as indicated above, the residual PEG and dead products derived from side reaction as impurities may be brought in the copolymer products [61,62], which have not been removed completely by re-precipitation. As a result, it can be seen that a shoulder was found at the low M_w side of GPC curves for various copolymers. Considering the very small content of PEG-based contaminants, their influence on the assembly behaviors in water of the copolymers should be not of importance, which was proved by experiment (see comparison study in Supplementary data Fig. S9).

The relatively small polydispersity indexes and the good correlation between the experimentally determined molar masses and the values obtained theoretically suggest that the polymerization proceeded in a more controlled fashion in the experimental conditions described above [61].

3.3. Aggregation behavior of the diblock copolymers

The amphiphilic PEG-*b*-PADMO copolymers readily self-assembled into micelle-like aggregates in water, and remained transparent solution except in the case of $E_{45}A_{88}$. ^{1}H NMR spectroscopy and a fluorescence probe technique were used to establish whether the copolymers were in the form of single molecules in water or self-associated into micelles with diameter smaller than the wavelength of visible light. Fig. 4 presents ^{1}H NMR spectra of the diblock copolymer $E_{45}A_{28}$ in deuterated acetone, D_2O and an acetone-d_6/D_2O mixture. Fig. 4a shows that the characteristic resonance signals of the dimethyl groups of PADMO (1.55 ppm) and PEG (about 3.60 ppm) were visible in acetone-d_6. As D_2O was added to acetone-d_6 the intensity of the sharp proton signals of the PADMO hydrophobic block was greatly reduced and broadened (Fig. 4b), and almost completely disappeared in neat D_2O (Fig. 4c), while the intensity of the PEG signal remained constant. These observations can be accounted for by the protons of PADMO chains becoming less mobile and less solvated in hydrophobic domains that formed in water. Thus we postulate the formation of micelle-like aggregates in water, with PADMO forming the compact hydrophobic core and PEG forming the solvated hydrophilic corona, as depicted schematically in Scheme 1.

The critical aggregation concentration (CAC) of the diblock copolymers PEG-*b*-PADMO was determined using pyrene as a fluorescent probe [64,65], whose fluorescent properties are sensitive primarily to the polarity of the microenvironment in which it is located. The ratio of intensity of 338 nm to 333 nm in the excitation spectrum would increase sharply if the polymers spontaneously aggregate, followed by pyrene probe transfer from water into the hydrophobic domains of the aggregates [66]. Plots of I_{338}/I_{333} versus copolymer concentration are displayed in Fig. 5. The I_{338}/I_{333} ratio remained almost constant in the low concentration region, and increased significantly upon further increasing the polymer concentration, indicating that the molecularly dissolved polymer chains began to associate into micelles and pyrene was partitioned into the less polar core. The CAC for PEG-*b*-PADMO copolymers with different compositions, determined from these plots are given in Table 1. The CAC values are comparable to those of other amphiphilic diblock copolymers such as PHPMAmDL-*b*-PEG (0.15–0.015 mg mL^{-1}) [67] and PLA-*b*-PEG (0.035–0.0025 mg mL^{-1}) [68], which should make the PEG-*b*-PADMO copolymers useful for pharmaceutical applications. As expected, the CAC values were significantly dependent on the length of the core-forming PADMO hydrophobic block. As the PADMO block length grew from $E_{45}A_{18}$ to $E_{45}A_{88}$, the CAC values decreased about two orders of magnitude, indicating sufficient hydrophobicity of the PADMO block to form micelles at very low concentration.

Table 1
Polymerization conditions and properties of diblock copolymers.

Sample	$[M]_0$ /$[CTA]_0$[a]	$M_{n(theor)} \times 10^{-4}$ (g mol^{-1})[b]	$M_{n(NMR)} \times 10^{-4}$ (g mol^{-1})[c]	$M_{n(GPC)} \times 10^{-4}$ (g mol^{-1})[d]	$M_{w(GPC)} \times 10^{-4}$ (g mol^{-1})[d]	PDI (M_w/M_n)[d]	CAC (mg mL^{-1})[e]
$E_{45}A_{18}$	20	0.54	0.51	0.47	0.53	1.13	0.120
$E_{45}A_{28}$	30	0.69	0.66	0.57	0.65	1.14	0.065
$E_{45}A_{47}$	50	1.00	0.96	0.81	0.92	1.13	0.029
$E_{45}A_{88}$	100	1.78	1.59	1.34	1.61	1.19	0.007

[a] $[M]_0/[CTA]_0$ is the ratio of initial concentration of monomer to PEG-CTA, while the ratio of concentration of PEG-CTA to initiator was kept at a constant value ($[CTA]_0/[I]_0 = 10$). Polymerization was performed in 1,4-dioxane at 70 °C for 24 h.
[b] Calculated from the equation, assuming that the reaction went to the completion.
[c] Determined from ^{1}H NMR spectra.
[d] Determined by GPC in THF, relative to linear polystyrene.
[e] The value of critical aggregates concentration (CAC) was estimated by a fluorescence spectroscopic method using pyrene as the fluorescence probe.

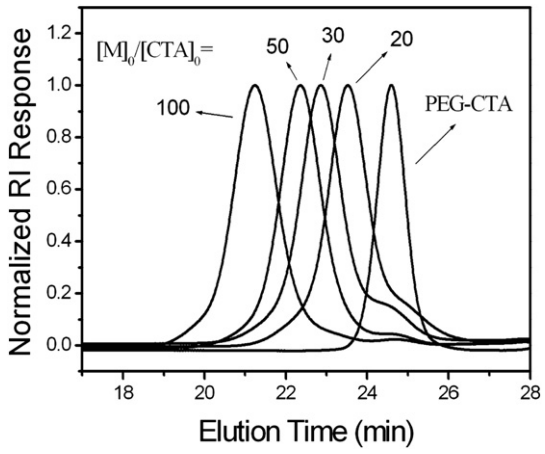

Fig. 3. GPC curves of PEG-CTA and the diblock copolymers PEG-*b*-PADMO obtained by RAFT polymerization at various $[M]_0/[CTA]_0$ ratios.

3.4. Sizes and morphologies

The hydrodynamic radius and distributions of the PEG-*b*-PADMO copolymers were measured in water by DLS at 1 mg mL^{-1} concentration, much higher than the CAC to ensure micelle formation. Fig. 6 shows a clear increase of particle size with increasing length of the PADMO block, and narrow size distribution. The copolymers $E_{45}A_{18}$ and $E_{45}A_{28}$ with shorter hydrophobic blocks showed similar behavior with a monomodal distribution and average hydrodynamic radius about 10 and 11 nm, respectively. $E_{45}A_{47}$ showed a bimodal distribution corresponding to average hydrodynamic radius 16 and 90 nm, indicating coexistence of two different aggregates, while $E_{45}A_{88}$, with the longest hydrophobic block, showed a monomodal distribution with radius about 129 nm. According to the calculation method in the literature [61], the theoretical maximum value of the radius of spherical micelles is 47 nm (for maximal chain stretching) for $E_{45}A_{88}$, taking the length of a C–C bond as 0.154 nm, and C–O bond as 0.143 nm respectively. Thus, it was thought that the polymer $E_{45}A_{88}$ may aggregate into shapes such as cylinders or vesicles, rather than spherical micelles.

The morphologies of the aggregates from the different block copolymers PEG-*b*-PADMO were visualized by TEM. Fig. 7 shows that the aggregates formed by $E_{45}A_{28}$ were spherical. $E_{45}A_{47}$ coexists as spherical and worm-like micelles, in accordance with the bimodal distribution found by DLS. The clear bilayer structure for $E_{45}A_{88}$ demonstrated formation of vesicles with radius about 100 nm. The difference in the diameters obtained by TEM and DLS was most probably due to shrinkage of the PEG shell upon drying, because DLS measurement was conducted in aqueous solution while TEM observation was on the collapsed state after evaporation of water. Consequently, the micellization behavior of the diblock PEG-*b*-PADMO copolymers clearly demonstrated that the small spherical micelles of $E_{45}A_{28}$ in aqueous solution transformed into worm-like micelles of $E_{45}A_{47}$ and into larger vesicles for $E_{45}A_{88}$, as the hydrophobic block length increased. These findings are in accordance with the general view that micelle morphology tends to change from spherical through rod-like or worm-like to a bilayer structure or vesicle, with increasing length of hydrophobic block, as for PS-*b*-PAA [69] and PLA-*b*-PEG [70].

It was of interest to find that the aqueous micelle solution of $E_{45}A_{47}$, at concentration higher than 2 mg mL^{-1}, was transparent at refrigerator (about 4 °C) and became cloudy at room temperature. This behavior was not observed for either the copolymers ($E_{45}A_{18}$ and $E_{45}A_{28}$), with shorter hydrophobic blocks or for $E_{45}A_{88}$ with a longer hydrophobic block, under the same conditions. This observation suggests that this type of block copolymer, with suitable composition, may exhibit thermally induced phase transition. This issue will be investigated elsewhere.

3.5. pH-responsive properties of diblock copolymer micelles

The PEG-*b*-PADMO diblock copolymers bearing acid-sensitive oxazolidine pendant groups were stable in neutral and basic

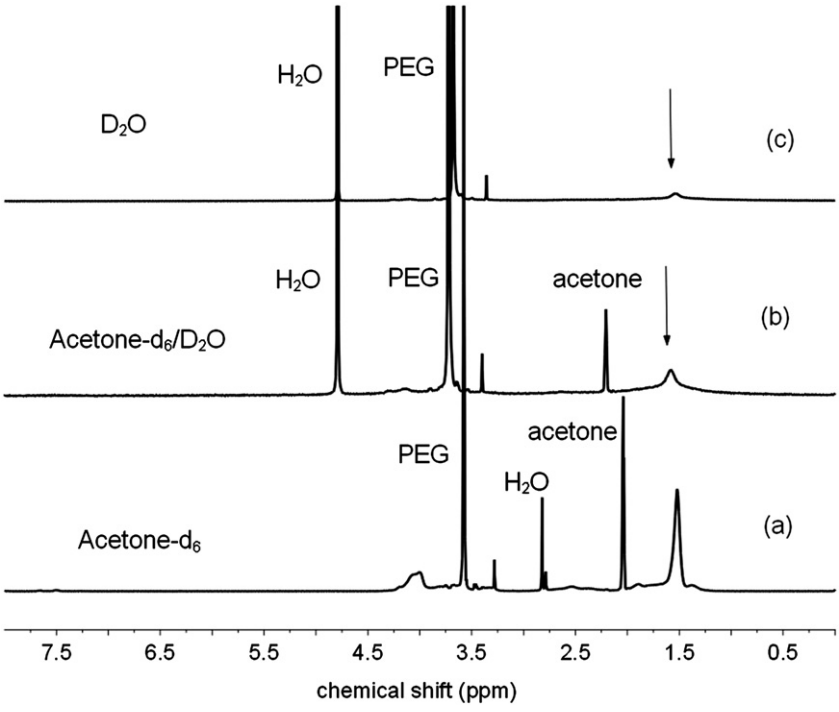

Fig. 4. ^1H NMR spectra of polymer $E_{45}A_{28}$ dissolved in (a) acetone-d_6; (b) mixture of acetone-d_6/D_2O (2/5 v/v); (c) D_2O.

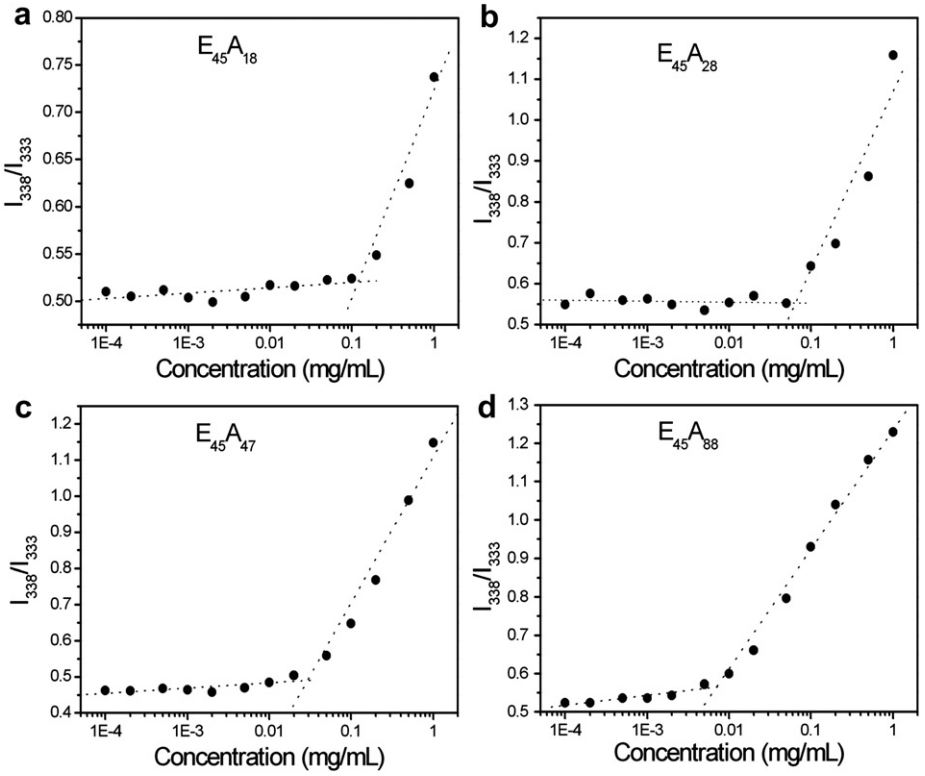

Fig. 5. I_{338}/I_{333} ratio for pyrene as a function of the logarithmic concentration of diblock copolymers.

conditions but easily hydrolyzed in acidic media. Upon hydrolytic cleavage of the five-membered ring, the hydrophobic part of the PADMO block is converted to hydrophilic poly(2-hydroxyethyl acrylamide) (PHEAM), thus causing disruption of the micelles.

To confirm hydrolytic cleavage of the oxazolidine groups of the copolymer in acid medium, an aqueous solution of copolymer $E_{45}A_{88}$ (1 mg mL^{-1}) was treated with 0.1 mol L^{-1} HCl at room temperature for 3 days. The micelle solution turned from cloudy to transparent, indicating dissociation. The resulting solution was dialyzed in a dialysis bag (MW cutoff 3500 Da) against water for three days, to remove small molecules and byproducts. After lyophilization, the macromolecular hydrolysis product was obtained as white powder that was readily soluble in water. ^{1}H NMR spectra of solutions in DMSO-d_6 of the copolymer before hydrolysis and the macromolecular product after complete hydrolysis, are shown in Fig. 8. The characteristic signals (1.55 ppm) of dimethyl groups of PADMO disappeared after hydrolysis, and new signals appeared at 7.50–8.00 and 4.50–5.00 ppm; these signals were assigned to the protons of imide and hydroxyl groups of PHEAM [71]. This result verified that the ADMO pendant groups were indeed accessible to hydrolysis by acid catalysis. As a result, the amphiphilic diblock PEG-*b*-PADMO copolymer was converted to the double hydrophilic diblock copolymer PEG-*b*-PHEAM in the acid environment, giving rise to concomitant dissociation of the micelles.

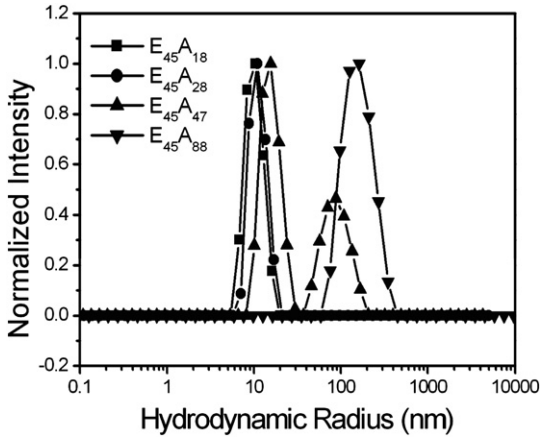

Fig. 6. Hydrodynamic radius distribution measured by DLS for the aqueous solutions of the four diblock copolymers. C_p = 1 mg mL^{-1}.

The size change of polymeric micelles in response to PADMO block hydrolysis was followed by DLS measurement. Fig. 9 shows the distribution of hydrodynamic radius of the micelles of copolymer $E_{45}A_{28}$ in pH 3.0 acetate buffer before and after hydrolysis. The micelles displayed a monomodal distribution prior to hydrolysis, with apparent hydrodynamic radius about 11 nm. The size of the micelles slowly decreased with hydrolysis time. Initially, the average size of the micelles increased to approximately 17 nm after 1 day: as a result of partial hydrolysis of the pendant oxazolidine groups, the micelle cores became increasingly hydrophilic and absorbed more water, leading to swelling of the micelles. As hydrolytic cleavage progressed, micelle disruption occurred via swelling and disintegration or dissociation, and a bimodal distribution appeared after 4 days. The new peak at about 2 nm can be attributed to single polymer chains, because the molecular weight of copolymer $E_{45}A_{28}$ was relatively small (about 6900 g mol^{-1}) [72]. Finally, after one week there was only one peak at about 1 nm. The reason was most probably the shrinking of the polymer coil by intramolecular hydrogen bonding between the amide and hydroxyl moieties as well as PEG units in the resulting PEG-*b*-PHEAM copolymer, because the HEAM units provided hydrogen for H-bonding (see Scheme 1). Similar results have been found for several polymers, including poly(hydroxyethyl methacrylate) [73,74] and polymethyacrylamide derivatives [49].

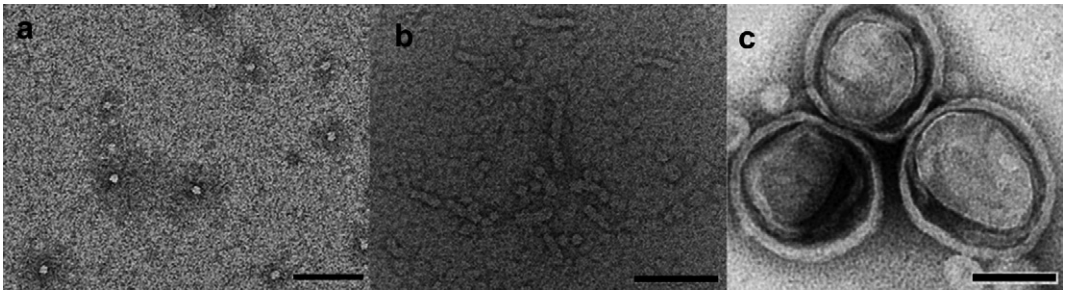

Fig. 7. TEM images of the aggregates formed by the diblock copolymers: (a) $E_{45}A_{28}$; (b) $E_{45}A_{47}$; (c) $E_{45}A_{88}$. The scale bars are 100 nm.

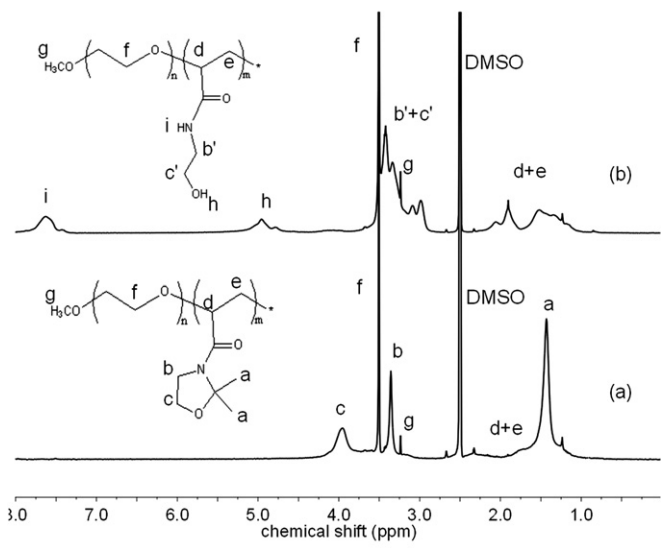

Fig. 8. ^{1}H NMR spectra of DMSO-d_6 solutions of (a) copolymer $E_{45}A_{88}$ before hydrolysis and (b) the product after complete hydrolysis.

The hydrolysis rates of micelles are commonly influenced by several factors. In addition to pH, temperature and ionic strength, the aggregate size and structure may play an important role that will strongly affect access of hydronium ions. The data from DLS given in section above provide the relevant information that the sizes of the micelles of PEG-*b*-PADMO copolymer increased from 10 to 129 nm as the length of the PADMO block increased from $E_{45}A_{18}$ to $E_{45}A_{88}$. To verify the micelle size and structure effect on reaction rate, hydrolysis of the oxazolidine groups of the PEG-*b*-PADMO copolymers was studied for the micelles of each copolymer in D_2O in the presence of DCl by monitoring, using ^{1}H NMR, the acetone generated from hydrolysis of the ADMO groups of the copolymer. The concentration of each block copolymer used for these experiments was 5 mg mL^{-1}, ensuring the formation of micelles. Fig. 10 shows typical ^{1}H NMR spectra for hydrolysis of copolymer $E_{45}A_{28}$. The characteristic signal of acetone (hydrolysis product) was found at 2.10 ppm and increased gradually with reaction time. Thus the extent of hydrolysis was calculated by comparing the acetone peak at 2.10 ppm with the peak at 3.38 ppm of terminal methyl protons of PEG, which did not change in the course of hydrolysis and was used as an internal standard. The kinetic data for each polymer are shown in Fig. 11.

The rate of hydrolysis was clearly dependent on the core-forming hydrophobic block length of PADMO, in the order $E_{45}A_{18} > E_{45}A_{28} > E_{45}A_{47}$. Since hydrolysis of oxazolidine moieties of copolymer took place within the micelle core, micelles with larger size and compact structure provided less accessibility of hydronium ions to the inner hydrophobic core of the micelles, thus strongly retarding hydrolytic cleavage of oxazolidine side groups.

3.6. pH-responsive release of Nile Red

The acid-sensitive destabilization of the micelles, which was expected to trigger release of a hydrophobic payload, was investigated using Nile Red (NR) as model substrate. NR is a hydrophobic

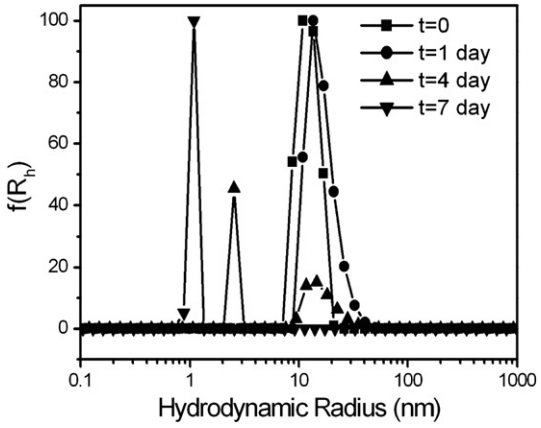

Fig. 9. Micelle hydrodynamic radius distributions at different hydrolysis times for $E_{45}A_{28}$ at pH 3.0, at 37 °C. $C_p = 1$ mg mL^{-1}.

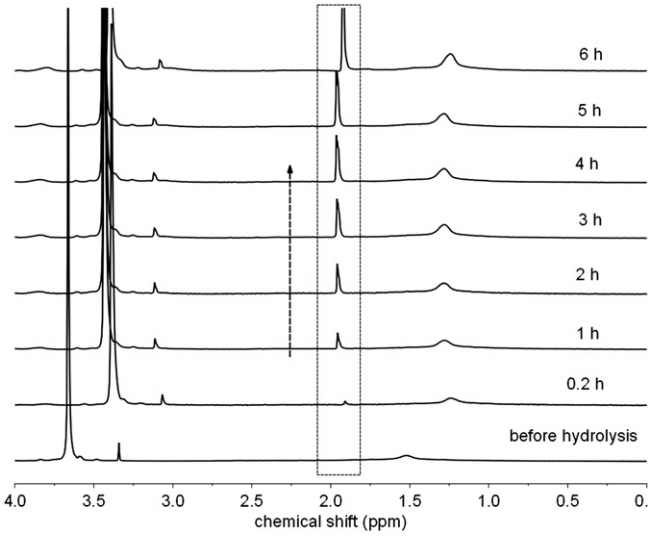

Fig. 10. ^{1}H NMR spectra at different reaction times for hydrolysis of polymer $E_{45}A_{28}$ in D_2O.

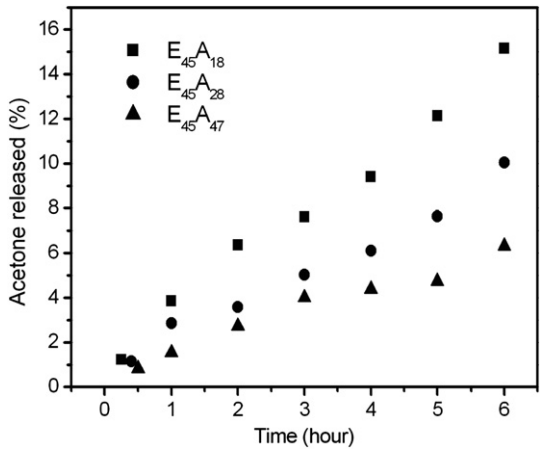

Fig. 11. Release of acetone as a function of hydrolysis time for polymer $E_{45}A_{18}$, $E_{45}A_{28}$, $E_{45}A_{47}$ in aqueous solutions, based on the data from ^{1}H NMR spectra.

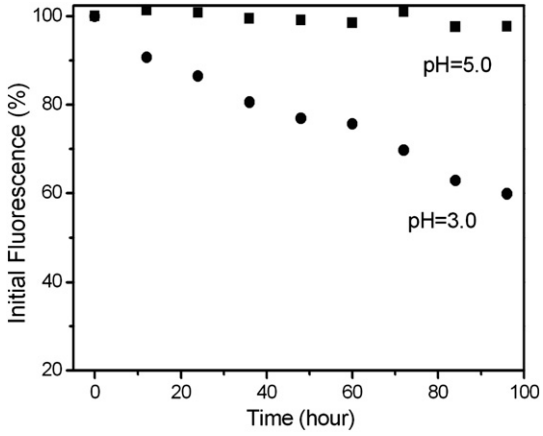

Fig. 12. Release profile of Nile Red from $E_{45}A_{28}$ micelles at pH 3.0 and 5.0 at 37 °C. C_p = 0.2 mg mL^{-1}.

dye frequently used as a fluorescence probe because its fluorescence is negligible in water, but is known to increase substantially in a hydrophobic environment such as the core of micelle [75]. When encapsulated NR is released from a micelle into water, its fluorescence is quenched. The release of NR as a result of the dissociation of polymer micelles in aqueous solution was monitored through fluorescence emission measurements. The results obtained from the micellar solution of $E_{45}A_{28}$ at different pHs are presented in Fig. 12. At pH 5.0, the fluorescence intensity of NR decreased very slowly as expected because of the low rate of hydrolysis of the oxazolidine as revealed by ^{1}H NMR spectra (Fig. 2). As pH was lowed to 3.0, the fluorescence intensity of NR rapidly decreased about 40% within 4 days. These observations are consistent with the results of ^{1}H NMR analysis, suggesting that the oxazolidine moieties of PEG-*b*-PADMO are indeed accessible and hydrolyzed in solutions of reduced pH, which leads to micelle disruption. The study showed that this type of pH-responsive polymer micelles can potentially be applied to triggered release of lipophilic drugs.

4. Conclusions

In this work, oxazolidine as a novel acid-sensitive functionality was exploited to construct a new type of stimuli-responsive polymer material, through copolymerization of oxazolidine derived monomer *N*-acryloyl-2,2-dimethyl-1,3-oxazolidine (ADMO). A series of novel pH-responsive diblock copolymers composed of fixed hydrophilic PEG block and various lengths of hydrophobic PADMO block were prepared by RAFT polymerization. The molecular weights obtained by ^{1}H NMR and GPC were close to the targeted theoretical data, suggesting the polymerization followed a controllable mechanism. The amphiphilic PEG-*b*-PADMO block copolymers prepared by RAFT polymerization easily self-assemble into micelle-like aggregates in water, with compact PADMO cores and solvated PEG coronas, at polymer concentrations above the CAC. The sizes and shapes of the polymeric micelles can be altered from spheres through worm-like structures to vesicles by increasing the PADMO block length. Under acid hydrolysis, the hydrophobic pendant oxazolidine groups are converted to water soluble β-hydroxyl amine derivative, leading to conversion of the amphiphilic PEG-*b*-PADMO copolymer to the double hydrophilic diblock copolymer PEG-*b*-PHEAM, followed by micelle disruption and release of loaded Nile Red. The hydrolysis rate of the copolymer micelles, demonstrated by ^{1}H NMR spectra, DLS, and fluorescence emission measurements of Nile Red, increases remarkably at acid pH and decreases with PADMO block length, due to the relatively large size and compact structure of the polymer micelles. Thus by utilizing the acid-labile PADMO segment as functional building block, it would be interesting to explore novel kinds of stimuli-responsive polymer materials and potential biotechnological applications. The other functionalities of oxazolidine based polymer materials, such as temperature responsive behavior, are currently under investigation in our group.

Appendix. Supplementary data

Supplementary data associated with this article can be found, free of charge, in the online version at doi:10.1016/j.polymer.2011.02.022.

References

[1] Mano JF. Adv Eng Mater 2008;10(6):515–27.
[2] Butsele KV, Jérôme R, Jérôme C. Polymer 2007;48:7431–43.
[3] Torchilin VP. Pharm Res 2007;24(1):1–16.
[4] Discher DE, Eisenberg A. Science 2002;297:967–73.
[5] Wei H, Yu CY, Chang C, Quan CY, Mo SB, Cheng SX, et al. Chem Commun; 2008:4598–600.
[6] Kim SY, Lee KE, Han SS, Jeong B. J Phys Chem B 2008;112:7420–3.
[7] Li X, Peng J, Wen Y, Kim DH, Knoll W. Polymer 2007;48:2434–43.
[8] Smith AE, Xu X, Abell TU, Kirkland SE, Hensarling RM, McCormick CL. Macromolecules 2009;42:2958–64.
[9] Maeda H, Wu J, Sawa T, Matsumura Y, Hori K. J Controlled Release 2000;65:271–84.
[10] Hawker CJ, Wooley KL. Science 2005;309:1200–5.
[11] Gohy JF, Willet N, Varshney S, Zhang J, Jérôme R. Angew Chem Int Ed 2001;40(17):3214–6.
[12] Talelli M, Rijcken CJF, Lammers T, Seevinck PR, Storm G, Nostrum CF, et al. Langmuir 2009;25:2060–7.
[13] Mitsukami Y, Hashidzume A, Yusa S, Morishima Y, Lowe AB, McCormick CL. Polymer 2006;47:4333–40.
[14] Wei H, Cheng SX, Zhang XZ, Zhuo RX. Prog Polym Sci 2009;34:893–910.
[15] Qian J, Wu FP. Chem Mater 2007;19:5839–41.
[16] Wang D, Wu T, Wan XJ, Wang XF, Liu SY. Langmuir 2007;23:11866–74.
[17] Wang YP, Zhang M, Moers C, Chen SL, Xu HP, Wang ZQ, et al. Polymer 2009;50:4821–8.
[18] Ma N, Li Y, Xu HP, Wang ZQ, Zhang X. J Am Chem Soc 2010;132:442–3.
[19] Fan HL, Huang J, Li YP, Yu JH, Chen JH. Polymer 2010;51:5107–14.
[20] Stenzel MH. Chem Commun; 2008:3486–503.
[21] Qian J, Wu FP. Chem Mater 2009;21:758–62.
[22] Mao BW, Gan LH, Gan YY, Tam KC, Tan OK. Polymer 2005;46:10045–55.
[23] Gillies ER, Fréchet JMJ. Chem Commun; 2003:1640–1.
[24] Murthy N, Thng YX, Schuck S, Xu MC, Fréchet JMJ. J Am Chem Soc 2002;124:12398–9.
[25] Chan Y, Bulmus V, Zareie MH, Byrne FL, Barner L, Kavallaris M. J Controlled Release 2006;115:197–207.
[26] Bulmus V, Chan Y, Nguyen Q, Tran HL. Macromol Biosci 2007;7:446–55.
[27] Zhang L, Bernard J, Davis TP, Barner-Kowollik C, Stenzel MH. Macromol Rapid Commun 2008;29:123–9.
[28] Themistou E, Patrickios CS. Macromol Chem Phys 2008;209:1021–8.

[29] Chan Y, Wong T, Byrne F, Kavallaris M, Bulmus V. Biomacromolecules 2008;9:1826–36.
[30] Lu JS, Li NJ, Xu QF, Ge JF, Lu JM, Xia XW. Polymer 2010;51:1709–15.
[31] Tang R, Palumbo RN, Ji WH, Wang C. Biomacomolecules 2009;10:722–7.
[32] Masson C, Garinot M, Mignet N, Wetzer B, Mailhe P, Scherman D, et al. J Control Release 2004;99:423–34.
[33] Heller J, Barr J, Ng SY, Abdellauoi KS, Gurny R. Adv Drug Deli Rev 2002;54: 1015–39.
[34] Bruyère H, Westwell AD, Jones AT. Bioorg Med Chem Lett 2010;20:2200–3.
[35] Lin S, Du FS, Wang Y, Ji SP, Liang DH, Yu L, et al. Biomacromolecules 2008;9: 109–15.
[36] Yang XQ, Grailer JJ, Pilla S, Steeber DA, Gong SQ. Bioconjug Chem 2010;21: 496–504.
[37] Lee YH, Park SY, Mok HJ, Park TG. Bioconjug Chem 2008;19:525–31.
[38] Hrubý M, Koňák C, Ulbrich K. J Control Release 2005;103:137–48.
[39] Burkoth AK, Anseth KS. Macromolecules 1999;32:1438–44.
[40] Ding CX, Gu JX, Qu XZ, Yang ZZ. Bioconjug Chem 2009;20:1163–70.
[41] Shi LJ, Berkland C. Macromolecules 2007;40:4635–43.
[42] Bae Y, Fukushima S, Harada A, Kataoka K. Angew Chem Int Ed 2003;42: 4640–3.
[43] Bae Y, Nishiyama N, Fukushima S, Koyama H, Yasuhiro M, Kataoka K. Bioconjug Chem 2005;16:122–30.
[44] Yoo HS, Lee EA, Park TG. J Control Release 2002;82:17–27.
[45] Oikawa M, Wada A, Okazaki F, Kusumoto S. J Org Chem 1996;61:4469–71.
[46] Deslongchamps P, Dory YL, Li S. Tetrahedron 2000;56:3533–7.
[47] Huang XN, Du FS, Zhang B, Zhao JY, Li ZC. J Polym Sci Part A Polym Chem 2008;46:4332–43.
[48] Huang XN, Du FS, Cheng J, Dong YQ, Liang DH, Ji SP, et al. Macromolecules 2009;42:783–90.
[49] Huang XN, Du FS, Liang DH, Lin SS, Li ZC. Macromolecules 2008;41:5433–40.
[50] Du FS, Huang XN, Chen GT, Lin SS, Liang DH, Li ZC. Macromolecules 2010;43:2474–83.
[51] Toncheva V, Schacht E, Ng SY, Barr J, Heller J. J Drug Target 2003;11(6):345–53.
[52] Tang RP, Ji WH, Wang C. Macromol Biosci 2010;10:192–201.
[53] Tessier A, Lahmar N, Pytkowicz J, Brigaud T. J Org Chem 2008;73:3970–3.
[54] Johansen M, Bundgaard H. J Pharm Sci 1983;72(11):1294–8.
[55] Mcclelland RA, Somani R. J Org Chem 1981;46:4345–50.
[56] Sélambarom J, Monge S, Carré F, Roque JP, Pavia AA. Tetrahedron 2002;58: 9559–66.
[57] Mitsukami Y, Donovan MS, Lowe AB, McCormick CL. Macromolecules 2001; 34:2248–56.
[58] Yusa S, Yokoyama Y, Morishima Y. Macromolecules 2009;42:376–83.
[59] Taylor WG, Hall TW, Schreck CE. Can J Chem 1992;70:165–72.
[60] Lowe AB, McCormick CL. Prog Polym Sci 2007;32:283–351.
[61] Garnier S, Laschewsky A. Macromolecules 2005;38:7580–92.
[62] Donovan MS, Lowe AB, Sanford TA, McCormick CL. J Polym Sci Part A Polym Chem 2003;41:1262–81.
[63] Jo YS, Vlies AJ, Gantz J, Antonijevic S, Demurtas D, Velluto D, et al. Macromolecules 2008;41:1140–50.
[64] Winnik FM. Chem Rev 1993;93:587–614.
[65] Wilhelm M, Zhao CL, Wang YC, Xu RL, Winnik MA. Macromolecules 1991;24: 1033–40.
[66] Bougard F, Giacomelli C, Mespouille L, Borsali R, Dubois P, Lazzaroni R. Langmuir 2008;24:8272–9.
[67] Soga O, Nostrum CF, Ramzi A, Visser T, Soulimani F, Frederik PM, et al. Langmuir 2004;20:9388–95.
[68] Hagan SA, Coombes AGA, Garnett MC, Dunn SE, Davies MC, Illum L, et al. Langmuir 1996;12:2153–61.
[69] Shen H, Eisenberg A. Macromolecules 2000;33:2561–72.
[70] Du B, Mei A, Yin K, Zhang Q, Xu J, Fan Z. Macromolecules 2009;42:8477–84.
[71] Narumi A, Chen Y, Sone M, Fuchise K, Sakai R, Satoh T, et al. Macromol Chem Phys 2009;210:349–58.
[72] Li WW, Matyjaszewski K, Albrecht K, Möller M. Macromolecules 2009;42: 8228–33.
[73] Weaver JVM, Bannister I, Robinson KL, Bories-Azeau X, Armes SP, Smallridge M, et al. Macromolecules 2004;37:2395–403.
[74] Eggenhuisen TM, Becer CR, Fijten MWM, Eckardt R, Hoogenboom R, Schubert US. Macromolecules 2008;41:5132–40.
[75] Jiang XG, Lavender CA, Woodcock JW, Zhao B. Macromolecules 2008;41: 2632–43.